JOURNAL OF SOLID STATE CHEMISTRY 90, 302–312 (1991)

The Crystal and Magnetic Structures of Ca_2NdRuO_6, Ca_2HoRuO_6, and Sr_2ErRuO_6

P. D. BATTLE* AND C. W. JONES

School of Chemistry, The University, Leeds, LS2 9JT, U.K.

AND F. STUDER

Laboratoire CRISMAT, Associé au CNRS-UA251, Campus II, Boulevard du Maréchal Juin, ISMRa, Université de Caen, 14042 Caen Cedex, France

Received July 23, 1990

The crystal structure of Sr_2ErRuO_6 has been refined from neutron powder diffraction data collected at room temperature; space group $P2_1/n$, $a = 5.7626(2)$, $b = 5.7681(2)$, $c = 8.1489(2)$ Å, $\beta = 90.19(1)°$. The structure is that of a distorted perovskite with a 1 : 1 ordered arrangement of Ru^{5+} and Er^{3+} over the 6-coordinate sites. Data collected at 4.2 K show the presence of long range antiferromagnetic order involving both Ru^{5+} and Er^{3+}. The temperature dependence of the sublattice magnetizations is described. The crystal structure of Ca_2NdRuO_6 is also that of a distored perovskite ($P2_1/n$, $a = 5.5564(1)$, $b = 5.8296(1)$, $c = 8.0085(1)$ Å, $\beta = 90.07(1)°$) with a random distribution of Ca^{2+} and Nd^{3+} on the A site and a 1 : 1 ordered arrangement of Ca^{2+} and Ru^{5+} on the 6-coordinate B sites. The Ru^{5+} sublattice is antiferromagnetic at 4.2 K but there is no evidence for magnetic ordering of the Nd^{3+} ions. Ca_2HoRuO_6 is also a distorted perovskite ($P2_1/n$, $a = 5.4991(1)$, $b = 5.7725(1)$, $c = 7.9381(2)$, $\beta = 90.18(1)°$ at 4.2 K) with a cation distribution best represented as $Ca_{1.46}Ho_{0.54}[Ca_{0.54}Ho_{0.46}Ru]O_6$. There is no ordering among the Ca^{3+} or Ho^{3+} ions on either the A or the B sites, but the Ca/Ho ions form a 1 : 1 ordered arrangement with Ru^{5+} on the B sites. At 4.2 K the Ru^{5+} ions adopt a Type I antiferromagnetic arrangement but there is no evidence of long range magnetic ordering among the Ho^{3+} ions.

Introduction

We have previously (*1–4*) described the magnetic properties of many compounds having the general formula $A_2BRu^{5+}O_6$, where A and B are diamagnetic cations. More recently (*5*) we have reported on the properties of Sr_2FeRuO_6 and $BaLaNiRuO_6$, two compounds which contain magnetic cations from both the first and the second transition series. The general aim of these studies has been to characterize the electronic properties of the Ru^{5+} cation, and to determine the extent to which the outer $4d^3$ electrons are delocalized. The magnetic behavior is a useful indicator of the degree of localization/delocalization in that a localized electron system is expected to show long-range magnetic order at low temperatures, whereas a delocalized system will not. Perovskite-related A_2BRuO_6 compounds have been found to order antiferro-

* To whom correspondence should be addressed at present address: Inorganic Chemistry Laboratory, South Parks Road, Oxford, OX1 3QR, U.K.

0022-4596/91 $3.00

magnetically with Néel temperatures (T_N) of 30 K and below (*1–4*). The observation of magnetic ordering in compounds containing second-row transition elements in high oxidation states is very unusual and the behavior of these materials presumably stems from the high correlation energy associated with the half-filled t_{2g} orbitals of 6-coordinate Ru^{5+} ($4d^3$: $^4A_{1g}$). Our study of Sr_2FeRuO_6 and $BaLaNiRuO_6$ was designed to monitor the magnetic interactions between Ru^{5+} and two electron configurations, Fe^{3+} : $3d^5$ and Ni^{2+} : $3d^8$, which were expected to be localized on the cations from the first transition series. We hoped that the superexchange coupling between d^3 and d^5 or d^8 ions might lead to ferromagnetism at low temperatures in these compounds but the positional cation ordering necessary for the observation of such behavior was unfortunately absent.

We have now turned our attention to the magnetic interactions between 4*d* and 4*f* electron systems, the latter clearly being localized. The variation in size of the trivalent ions of the different rare-earth elements leads to a number of interesting structural possibilities in perovskites. The larger rare-earths will occupy the *A* sites, ideally 12-coordinate in an undistorted perovskite, whereas the smaller lanthanides may occupy the 6-coordinate *B* site. The parameter which defines whether a particular cation is classified as "large" or "small" is the relative size of the rare earth ion compared to that of the other cations present. Thus it is possible to prepare compounds with different concentrations of rare-earth ions on the 6-coordinate site, for example in Ba_2LaRuO_6 the lanthanum atoms are all octahedrally coordinated on the B site whereas in Ca_2LaRuO_6, more correctly written as $CaLa[CaRu]O_6$, they occupy half the *A* sites (*1*). Ca_2YRuO_6 (*3*), better written as $Ca_{1.43}Y_{0.57}[Yo_{0.43}Ca_{0.57}Ru]O_6$, is an example of an intermediate case. An array of lanthanide ions on the 6-coordinate B site of a perovskite can order antiferromagnetically at relatively high temperatures, for example T_N = 37 K for $BaTbO_3$ (*6*). However, this is not always the case, as for example in $BaPrO_3$ where $T_N < 2$ K (*6*). When the lanthanide ions occupy only the *A* site, they tend to order magnetically at very low temperatures, for example 4.3 K in $ErFeO_3$ (*7*), even if the *B* sites are occupied by ions from the first transition series, which order magnetically at much higher temperatures (620 K in $ErFeO_3$). In this paper we describe the synthesis and characterization of Sr_2ErRuO_6, Ca_2NdRuO_6, and Ca_2HoRuO_6. These three compositions were chosen in an attempt to produce compounds having respectively all, none, and a fraction of the lanthanide ions on 6-coordinate sites. We have performed neutron powder diffraction experiments to determine the nature of any magnetic coupling between the rare-earth and the transition metal cations in each case.

Experimental

Polycrystalline samples of the title compounds were prepared by firing the appropriate quantities of $SrCO_3$, $CaCO_3$, Er_2O_3, Ho_2O_3, and Nd_2O_3 (all Johnson Matthey Chemicals) in air at temperatures of up to 1300°C (Sr_2ErRuO_6) or 1100°C (Ca_2NdRuO_6 and Ca_2HoRuO_6) for a period of several days. The mixtures were ground and remade into pellets several times during the course of the reactions, the progress of which was monitored by X-ray powder diffraction. This technique indicated that the final products were monophasic, perovskite-like compounds with symmetries lower than cubic. Magnetic susceptibility data were collected in the temperature range $80 < T < 300$ K using a Newport Instruments Gouy balance. Magnetization measurements were made at 4.2 K using a vibrating sample magnetometer. Neutron powder diffraction data were collected on

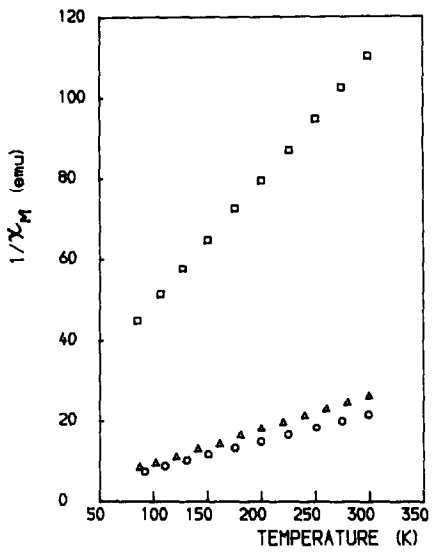

FIG. 1. The inverse molar magnetic susceptibilities of Sr_2ErRuO_6 (Δ), Ca_2HoRuO_6 (O), and Ca_2NdRuO_6 (□) as a function of temperature.

Sr_2ErRuO_6 at temperatures of 4.2, 10, 20, 30, 40, and 295 K using the diffractometer D2b at ILL Grenoble, operating with a mean neutron wavelength of 1.594 Å. The diffractometer D1a (λ = 1.909 Å) was used to collect data on Ca_2NdRuO_6 at room temperature and 4.2 K, and on Ca_2HoRuO_6 at 4.2 K only. In all cases the samples were contained in vanadium cans and data were collected at 2θ intervals of 0.05° over the angular range $0 < 2\theta < 160°$.

Results

(*i*) *High Temperature Magnetic Susceptibilities*

The variation of the inverse molar magnetic susceptibility with temperature is shown in Fig. 1 for Sr_2ErRuO_6, Ca_2NdRuO_6, and Ca_2HoRuO_6. The values of the average effective magnetic moment per cation (μ_{eff}) and the Weiss constant (θ) derived by fitting the data to a Curie-Weiss Law are listed in Table I.

(*ii*) *Crystal Structures*

All the neutron diffraction data collected in this study were analyzed by the Rietveld (*8*) profile analysis technique using the following scattering lengths: $b_{Sr} = 0.69$, $b_{Ca} = 0.47$, $b_{Er} = 0.79$, $b_{Nd} = 0.75$, $b_{Ho} = 0.85$, $b_{Ru} = 0.73$, and $b_O = 0.58 \times 10^{-12}$ cm. The background levels were estimated by interpolation between regions of the diffraction pattern where there were no Bragg peaks, and all the latter were assumed to have a Gaussian line profile.

The neutron diffraction data collected on Sr_2ErRuO_6 at room temperature could be indexed in a monoclinic unit cell with $a = 5.7626(2)$, $b = 5.7681(2)$, $c = 8.1489(2)$ Å, $\beta = 90.19(1)°$, and space group $P2_1/n$. The unit cell is related to the primitive perovskite unit cell in the following way: $a \approx \sqrt{2}a_p$, $b \approx \sqrt{2}a_p$, $c \approx 2a_p$. This type of unit cell, part of which is illustrated in Fig. 2, has been found in many Ru^{5+} compounds (*1–4*); the space group $P2_1/n$ allows two crystallographically distinct octahedral sites in the perovskite structure, thus permitting 1 : 1 positional ordering between Ru^{5+} and the other 6-coordinate cation, *B*. The crystal structure of Sr_2ErRuO_6 was refined with an ordered arrangement of Ru and Er on the octahedral sites. After the exclusion of the asymmetric peaks having $2\theta < 30°$, refinement of the usual profile parameters and eighteen atomic parameters gave the following agreement factors: R_{wp}

TABLE I

MAGNETIC PARAMETERS OF Sr_2ErRuO_6, Ca_2HoRuO_6 AND Ca_2NdRuO_6

Compound	θ (K)	$\langle\mu_{eff}\rangle$ (μ_B)[a]
Sr_2ErRuO_6	−12(1)	6.87(5)
Ca_2HoRuO_6	−15(1)	7.66(5)
Ca_2NdRuO_6	−60(2)	3.62(5)

[a] The average effective magnetic moment per paramagnetic ion.

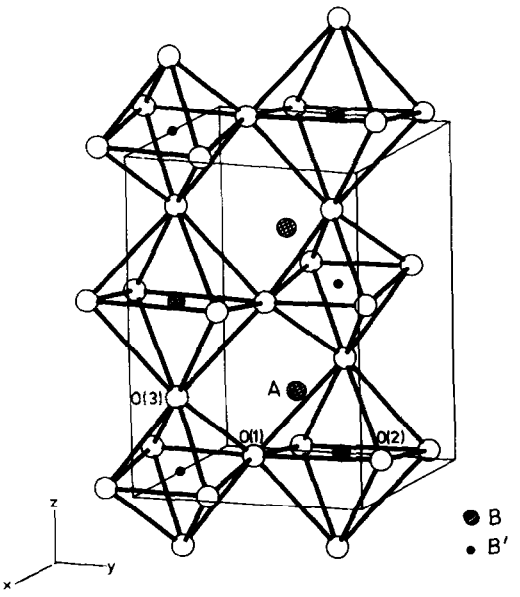

FIG. 2. The crystal structure of an ordered perovskite A_2BRuO_6 (B′ = Ru).

= 8.08%, R_I = 3.18%. The final observed, calculated, and difference diffraction profiles are plotted in Fig. 3 and the refined atomic parameters and the more important bond lengths and bond angles are listed in Tables II and III, respectively. The diffraction data collected on Sr_2ErRuO_6 at a temperature of 4.2 K contained a number of low-angle peaks which were not observed at room temperature, and thus indicated that this compound exhibits long-range magnetic order at low temperatures. There were more such peaks than we have observed previously (*1–4*) in experiments on perovskites having the general formula A_2BRuO_6, where *A* and *B* are diamagnetic cations, and the total intensity of the magnetic scattering was also increased. We therefore concluded that both the Ru^{5+} and the Er^{3+} ions are magnetically ordered in Sr_2ErRuO_6 at 4.2 K. Most of the A_2BRuO_6 compounds studied to date order as Type I antiferromagnets. This magnetic structure

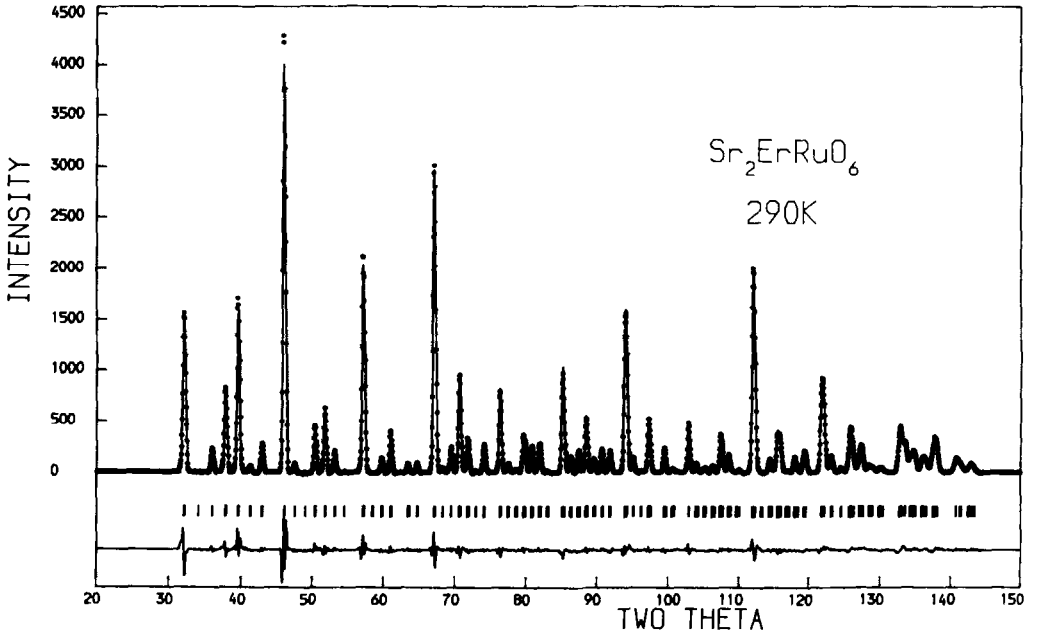

FIG. 3. The observed, calculated, and difference neutron powder diffraction profiles of Sr_2ErRuO_6 at room temperature. Reflection positions are marked.

TABLE II

STRUCTURAL PARAMETERS FOR Sr_2ErRuO_6 AT ROOM TEMPERATURE (SPACE GROUP $P2_1/n$)

Atom	Site	x	y	z	B (Å^2)
Sr	4e	0.0065(8)	0.0256(4)	0.2482(7)	0.73(3)
Er	2d	$\frac{1}{2}$	0	0	0.50(4)
Ru	2c	$\frac{1}{2}$	0	$\frac{1}{2}$	0.48(5)
O1	4e	0.2672(7)	0.2964(7)	0.0339(6)	0.84(8)
O2	4e	0.2021(8)	−0.2303(8)	0.0332(5)	0.89(7)
O3	4e	−0.0670(7)	0.4876(6)	0.2365(4)	0.84(5)

type is most easily envisaged in a pseudocubic unit cell of size $\sim 2a_p \times 2a_p \times 2a_p$, such that the Ru^{5+} ions form a face-centered array, as shown in Fig. 4. Ferromagnetic sheets parallel to the xy plane are stacked antiferromagnetically along the $\hat{z}$ axis, such that each cation is coupled ferromagnetically to four of its twelve nearest neighbors and antiferromagnetically to the remaining eight. The magnetic structure used to model the behavior of Sr_2ErRuO_6 is illustrated in Fig. 5. In a $2a_p \times 2a_p \times 2a_p$ unit cell, the Er^{3+} and Ru^{5+} ions form two interpenetrating face-centered sublattices. Each of these orders magnetically in a Type I arrangement, but in any given xy sheet the Er^{3+} and Ru^{5+} magnetic moments are coupled ferrimagnetically rather than ferromagnetically. The resultant magnetic structure is similar to C-type ordering on a primitive cubic lattice in that it results in ferromagnetic (110) cation sheets (*9*). To verify our model we performed a simultaneous refinement of the crystal and magnetic structures of Sr_2ErRuO_6 by profile analysis. This involved the variation of the ordered component of the magnetic moment of the Er^{3+} and Ru^{5+} ions in addition to the parameters used in the analysis of the room temperature data set. It also involved the choice of form factor curves to describe the angular dependence of the magnetic scattering. The magnetic scattering observed in our previous experiments on Ru^{5+} mixed metal oxides was very weak, and we always felt justified in estimating the magnetic moment per Ru^{5+} cation from the intensity of the only strong magnetic Bragg peak, thus avoiding any errors due to the use of an inaccurate, empirical form factor. However, the additional complexity introduced by the presence of a second magnetic species made it necessary to use full profile analysis in the case of Sr_2ErRuO_6. We therefore deduced a form factor for Ru^{5+} by taking that reported for the isoelectronic species Mo^{3+} (*10*) and expanding it by an

TABLE III

SELECTED BOND LENGTHS (IN Å) AND BOND ANGLES (IN DEGREES) FOR Sr_2ErRuO_6 AT ROOM TEMPERATURE

Er–O1	2.191(8) × 2	Ru–O1	1.955(8) × 2
Er–O2	2.188(8) × 2	Ru–O2	1.962(8) × 2
Er–O3	2.181(7) × 2	Ru–O3	1.968(7) × 2

Sr–O1	Sr–O2	Sr–O3
2.79(1)	2.56(1)	2.70(1)
2.57(1)	2.84(1)	2.55(1)
2.90(1)	2.82(1)	

O1–Er–O2	91.3	O1–Ru–O2	90.6
O1–Er–O3	90.5	O1–Ru–O3	90.2
O2–Er–O3	90.3	O2–Ru–O3	90.7

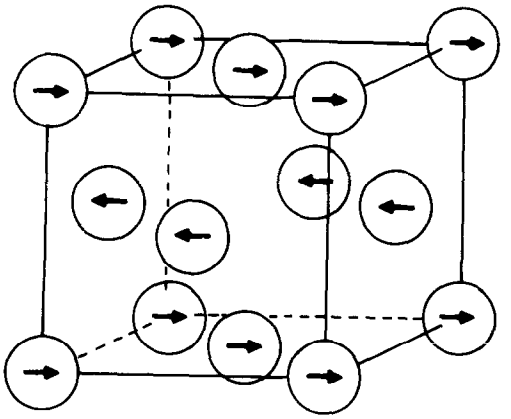

FIG. 4. Type I spin arrangement in antiferromagnetic A_2BRuO_6. Only the Ru^{5+} ions are marked; they occupy half the octahedral sites of the perovskite structure.

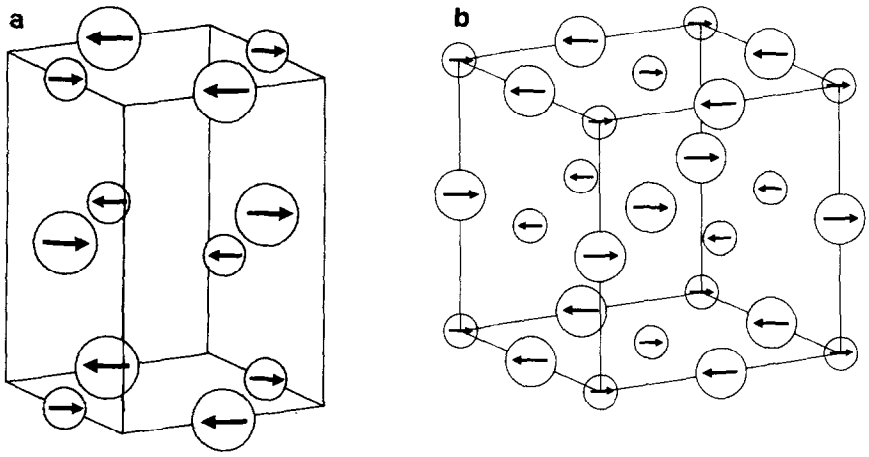

FIG. 5. The magnetic structure of Sr_2ErRuO_6, (a) in a unit cell of size $\sqrt{2}a_p \times \sqrt{2}a_p \times 2a_p$, (b) in a unit cell of size $2a_p \times 2a_p \times 2a_p$. Diamagnetic ions are omitted. Larger circles Er^{3+}; smaller circles Ru^{5+}.

amount appropriate for an increase of two units in the ionic charge. The form factor of Er^{3+} was calculated using the method of Blume *et al.* (*11*). Our refinements then converged to agreement factors of R_{wpr} = 8.58%, R_I = 2.75% when the atomic magnetic moments were aligned along $\hat{x}$. The final diffraction profiles are shown in Fig. 6 and the corresponding structural parameters are tabulated in Table IV. Diffraction data were collected at temperatures above 4.2 K in order to monitor the temperature dependence of the ordered cation magnetic moments. These data were analyzed fully by the Rietveld method (*12*) and the resulting values of the magnetic moments are plotted in Fig. 7. In our neutron data analysis we assumed that all the atomic magnetic moments were collinear, and the good agreement between our observed and calculated diffraction profiles suggests that this is a reasonable assumption. However, our magnetometer measurements revealed a small (ca. $0.7\mu_B$ per formula unit) remanent magnetisation and we must recognize that in the analysis of our neutron data, we have failed to allow for a slight canting of the magnetic moments. A single crystal sample will be needed if this effect is to be described accurately. Our results showed that Sr_2ErRuO_6 is paramagnetic at a temperature of 50 K.

TABLE IV

STRUCTURAL PARAMETERS FOR Sr_2ErRuO_6 AT 4.2 K (SPACE GROUP $P2_1/n$)

Atom	Site	x	y	z	B (Å^2)	μ_x (μ_B)
Sr	4e	0.0079(6)	0.0305(3)	0.2498(6)	0.24(2)	
Er	2d	$\frac{1}{2}$	0	0	0.25(4)	4.59(3)
Ru	2c	$\frac{1}{2}$	0	$\frac{1}{2}$	0.35(4)	1.74(6)
O1	4e	0.2676(6)	0.2990(6)	0.0356(6)	0.46(7)	
O2	4e	0.1984(6)	−0.2293(6)	0.0354(5)	0.37(6)	
O3	4e	−0.0696(6)	0.4865(5)	0.2354(4)	0.44(4)	

Note. a = 5.7500(2), b = 5.7636(2), c = 8.1354(3) Å, β = 90.22(1).

The neutron diffraction data collected on Ca_2NdRuO_6 at room temperature could also be indexed in space group $P2_1/n$ with a = 5.5564(1), b = 5.8296(1), c = 8.0085(1) Å, β = 90.07(1)° and we therefore initially assumed that the crystal structure of this compound was similar to that described above for Sr_2ErRuO_6. However, during the initial stages of the structure refinement it became apparent that Nd occupies only the

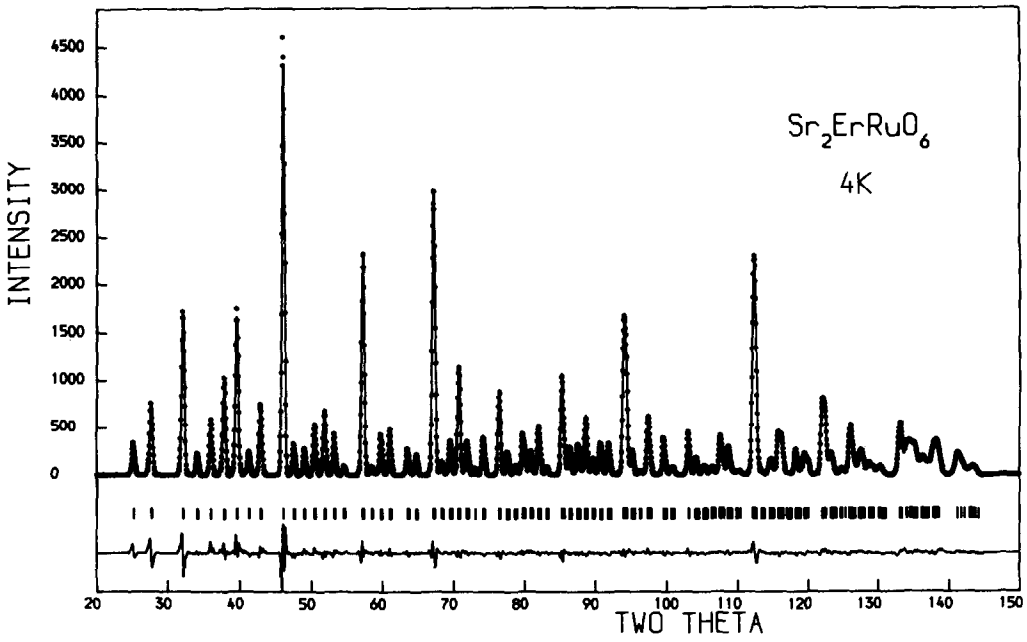

FIG. 6. The observed, calculated, and difference neutron powder diffraction profiles of Sr_2ErRuO_6 at 4.2 K. Reflection positions are marked.

A site in this material, which is thus more properly formulated as $CaNd[CaRu]O_6$. The cation distribution was held fixed during our final refinements, which resulted in the structural parameters listed in Table V and the bond lengths and bond angles given in Table VI. There was no evidence for ordering between Nd^{3+} and Ca^{2+} on the *A* sites. The observed and calculated neutron diffraction profiles are plotted in Fig. 8; the corresponding *R*-factors are $R_{wpr} = 8.55\%$, $R_I = 4.73\%$. The data collected at 4.2 K contained weak additional Bragg scattering at a low angle. The positions and intensities of these peaks suggested that the Ru sublattice of Ca_2NdRuO_6 shows Type I antiferromagnetism at 4.2 K, with no long range magnetic ordering of the Nd atoms on the *A*

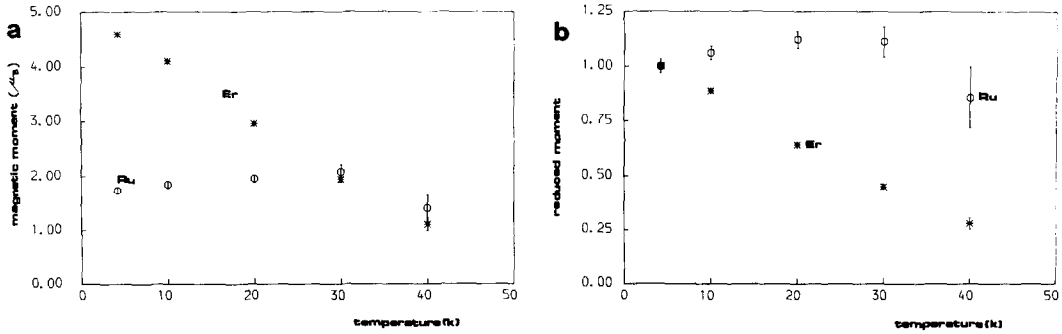

FIG. 7. The temperature dependence of the sublattice magnetizations in Sr_2ErRuO_6, (a) plotted as magnetic moment per cation, (b) normalized to the value of the magnetic moment at 4.2 K.

TABLE V

STRUCTURAL PARAMETERS FOR Ca_2NdRuO_6 AT ROOM TEMPERATURE (SPACE GROUP $P2_1/n$)

Atom	Site	x	y	z	B (Å^2)
Ca/Nd	4e	0.5145(3)	0.5590(2)	0.2545(4)	0.49(3)
Ca	2c	0	$\frac{1}{2}$	0	0.63(9)
Ru	2d	$\frac{1}{2}$	0	0	0.51(6)
O1	4e	0.2131(4)	0.1762(4)	−0.0514(4)	0.70(5)
O2	4e	0.3280(4)	0.7198(4)	−0.0664(3)	0.85(6)
O3	4e	0.3882(3)	−0.0494(4)	0.2291(3)	0.68(4)

TABLE VI

SELECTED BOND LENGTHS (IN Å) AND BOND ANGLES (IN DEGREES) FOR Ca_2NdRuO_6 AT ROOM TEMPERATURE

Ca–O1	2.266(4) × 2	Ru–O1	1.940(4) × 2
Ca–O2	2.291(5) × 2	Ru–O2	1.965(5) × 2
Ca–O3	2.274(4) × 2	Ru–O3	1.959(4) × 2

Ca/Nd–O1	Ca/Nd–O2	Ca/Nd–O3
2.707(6)	2.925(6)	2.397(5)
2.347(6)	2.383(6)	2.329(5)
2.779(6)	2.598(6)	

O1–Ca–O2	90.4	O1–Ru–O2	90.9
O1–Ca–O3	94.3	O1–Ru–O3	90.9
O2–Ca–O3	94.4	O2–Ru–O3	91.3

sites. We therefore analyzed these data using the same method as in our previous work (*1–4*), that is we refined the crystal structure by profile analysis and then calculated the ordered magnetic moment per Ru^{5+} by comparing the intensity of the only strong magnetic peak to those of the nuclear peaks. The (001) magnetic peak occurs at $\sin\theta/\lambda \approx 0.06$ and we therefore assumed a value of unity for the form factor at this scattering angle. We prefer to use this approach, with its clear limitations, rather than to introduce uncertainty by attempting to model the intensities of a small number of weak magnetic peaks using an empirical form factor. Our calculations led to a value of $1.5(2)\mu_B$ for the ordered magnetic moment per Ru^{5+} ion. The structural parameters resulting from profile analysis of the 4.2 K data set are listed in Table VII; the corresponding R-factors are $R_{wpr} = 8.21\%$, $R_I = 4.99\%$.

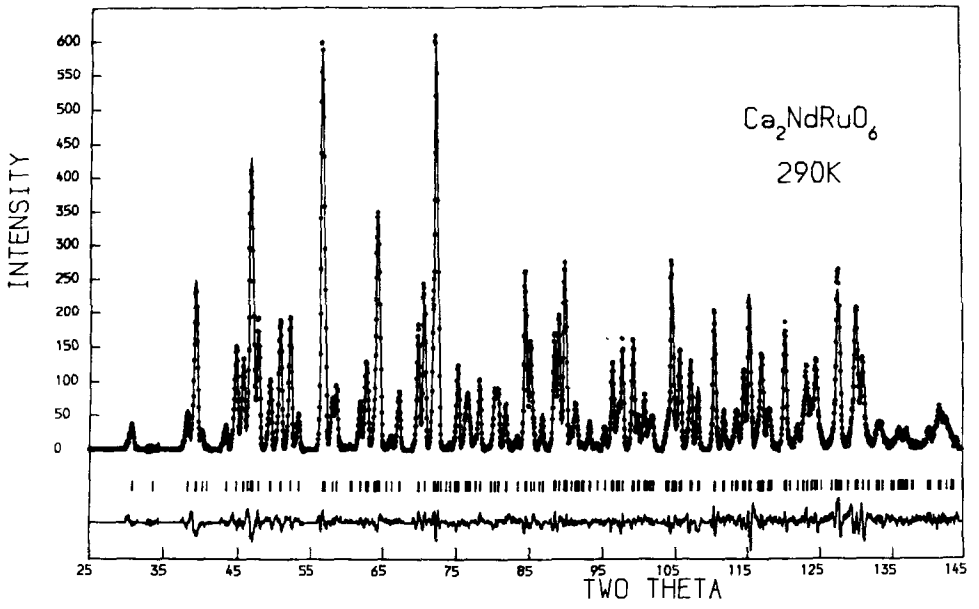

FIG. 8. The observed, calculated, and difference neutron powder diffraction profiles of Ca_2NdRuO_6 at room temperature. Reflection positions are marked.

TABLE VII

STRUCTURAL PARAMETERS FOR Ca_2NdRuO_6 AT 4.2 K (SPACE GROUP $P2_1/n$)

Atom	Site	x	y	z	B (Å^2)
Ca/Nd	4e	0.5160(3)	0.5612(2)	0.2545(4)	0.10(3)
Ca	2c	0	½	0	0.18(8)
Ru	2d	½	0	0	0.47(5)
O1	4e	0.2132(4)	0.1773(4)	−0.0523(3)	0.43(5)
O2	4e	0.3287(4)	0.7185(4)	−0.0671(3)	0.45(5)
O3	4e	0.3877(3)	−0.0501(3)	0.2291(3)	0.42(4)

Note. a = 5.5439(1), b = 5.8282(1), c = 7.9931(1) Å, β = 90.06(1)°.

TABLE VIII

STRUCTURAL PARAMETERS FOR Ca_2HoRuO_6 AT 4.2 K (SPACE GROUP $P2_1/n$)

Atom	Site	x	y	z	B (Å^2)
Ca/Ho1	4e	0.5167(4)	0.5620(3)	0.2555(4)	0.22(4)
Ca/Ho2	2c	0	½	0	0.22(4)
Ru	2d	½	0	0	0.34(6)
O1	4e	0.2123(4)	0.1788(5)	−0.0545(4)	0.45(5)
O2	4e	0.3277(4)	0.7182(4)	−0.0678(4)	0.32(6)
O3	4e	0.3835(4)	−0.0518(4)	0.2303(4)	0.42(4)

Note. Site occupancies: Ca/Ho1 73.0(4)%Ca; 27.0(4)% Ho
Ca/Ho2 54.0(4)%Ca; 46.0(4)% Ho.

The neutron diffraction data collected on Ca_2HoRuO_6 at 4.2 K could be interpreted using a monoclinic unit cell having a = 5.4991(1), b = 5.7725(1), c = 7.9381(2) Å, β = 90.18(1)° and space group $P2_1/n$. We refined the crystal structure as a distorted perovskite, allowing the distribution of Ho and Ca over the A and B sites to vary. As in the case of Ca_2NdRuO_6, weak magnetic peaks were observed at low angles, and these were again excluded from the profile analysis, which converged at the following R-factors: R_{wpr} = 7.55%, R_I = 4.28%. The refined structural parameters are listed in Table VIII and selected bond lengths and bond angles are presented in Table IX. The observed and calculated diffraction profiles are drawn in Fig. 9. The distribution of magnetic scattering was again suggestive of Type I antiferromagnetic ordering of the Ru^{5+} ions, with no indication of magnetic order among the Ho^{3+} ions on either the A

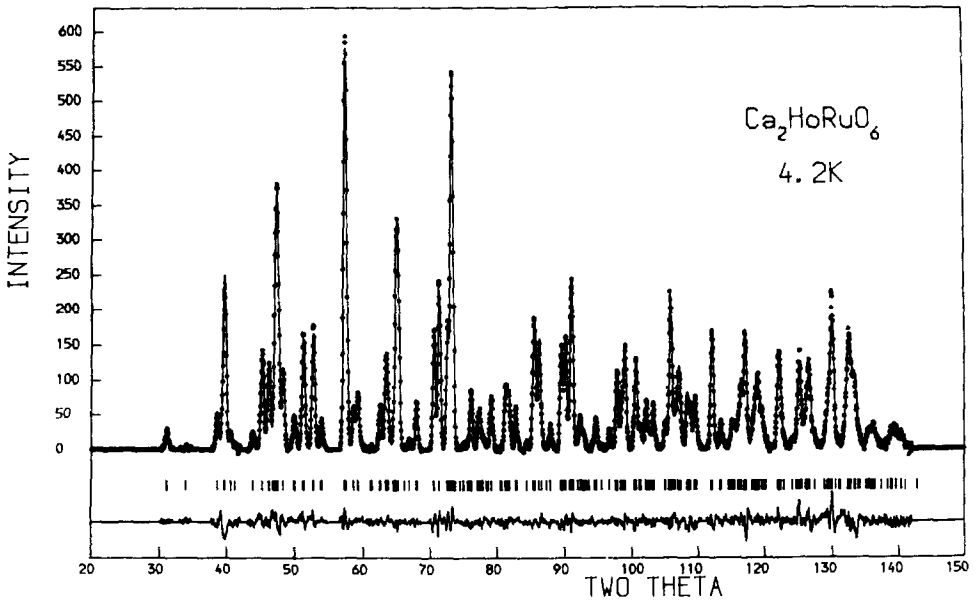

FIG. 9. The observed, calculated, and difference neutron powder diffraction profiles of Ca_2HoRuO_6 at 4.2 K. Reflection positions are marked.

TABLE IX

SELECTED BOND LENGTH (IN Å) AND BOND ANGLES (IN DEGREES) FOR Ca_2HoRuO_6 AT 4.2 K

Ca/Ho2–O1	2.234(5) × 2	Ru–O1	1.938(5) × 2
Ca/Ho2–O2	2.264(4) × 2	Ru–O2	1.958(4) × 2
Ca/Ho2–O3	2.253(4) × 2	Ru–O3	1.962(4) × 2

Ca/Ho1–O1	Ca/Ho1–O2	Ca/Ho1–O3
2.650(6)	2.361(6)	2.355(6)
2.313(6)	2.546(6)	2.300(6)
2.774(6)		

O1–Ca/Ho2–O2	90.05	O1–Ru–O2	90.76
O1–Ca/Ho2–O3	94.19	O1–Ru–O3	91.17
O2–Ca/Ho2–O3	94.36	O2–Ru–O3	91.70

sites or the *B* sites. A comparison of the intensity of the (001) magnetic peak with those of other peaks led to a value of $1.4(6)\mu_B$ for the ordered component of the Ru^{5+} magnetic moment.

Discussion

The negative values of the Weiss constants (θ) listed in Table I indicate that the predominant magnetic interactions in all of the three compounds under consideration are antiferromagnetic. Our susceptibility data only give a measure of the average effective magnetic moment per cation; we are unable to derive a value of μ_{eff} for Ru^{5+} from our results and we are thus unable to use the high-temperature susceptibility behavior as an indication of the degree of delocalization of the $4d^3$ electron configuration, as has been possible in our previous work (*1–4*).

The crystal structure of Sr_2ErRuO_6 is unremarkable in the light of our previous work (*4*) on Sr_2LuRuO_6. The compound adopts a distorted perovskite structure, where the distortion can be thought of as arising from the rotation of essentially regular octahedra rather than from the presence of a wide range of Ru–O or Er–O bond lengths. The magnetic structure adopted by Sr_2ErRuO_6 is more interesting. The description of the ordering as two interpenetrating face-centered Type I antiferromagnetic sublattices implies that the antiferromagnetic superexchange between pairs of nearest like neighbors is a strong interaction. This is reasonable in the case of Ru^{5+}, for which such behavior has been seen in, for example, Sr_2LuRuO_6, but it is less likely to be a realistic description of the magnetic coupling between Er^{3+} ions. The latter usually couple only very weakly, even when separated by only one diamagnetic atom as in Er_2O_3 which has a Néel temperature of 3.4 K (*13*). The likely order of interaction strength in Sr_2ErRuO_6 is Ru–Ru > Ru–Er > Er–Er. The description of the magnetic structure of Sr_2ErRuO_6 as a C-type structure is then more attractive. This type of magnetic ordering involves strong antiferromagnetic coupling not only between nearest-neighbor cations on a primitive lattice, but also between next-nearest-neighbor cations, such that each ion is antiferromagnetically coupled to four out of six nearest neighbors and eight out of twelve next-nearest-neighbors. We envisage that Type I Ru–Ru coupling initiates the onset of long range magnetic order in this material, and that antiferromagnetic superexchange between Ru^{5+} and Er^{3+} causes the latter to follow, resulting in a structure that can be described as C-type if we ignore the fact that two different types of ion are involved. The apparent Type I order on the Er^{3+} sublattice is thus an inevitable consequence of the Ru–Ru and Ru–Er coupling, rather than a direct result of Er–Er interactions. The proposed sequence of interaction strengths is consistent with the observed temperature dependence of the ordered cation magnetic moments, that of the Er^{3+} ions falling off much more rapidly with increasing temperature than that of the Ru^{5+} ions. The observed saturation moment of the latter ($1.74\mu_B$) is within the range of values reported (*1–4*) for other magnetically ordered

compounds containing the same cation. The data in Fig. 7 suggest that the Er^{3+} sublattice is not magnetically saturated at 4.2 K.

The unit cell parameters of Ca_2NdRuO_6 and Ca_2HoRuO_6 show a much greater departure from cubic symmetry than do those of Sr_2ErRuO_6. This increased distortion is also apparent in the values of the refined atomic coordinates and the bond lengths and bond angles listed in Tables VI and IX. The presence of a smaller cation on the *A* site leads to a greater degree of rotation of the BO_6 octahedra and to a greater range of bond distances and bond angles within the individual octahedra. The other consequence of the replacement of Sr by Ca is that the rare-earth cations move, to some extent, from the *B* site to the *A* site, with the alkaline earth occupying the 6-coordinate *B* site. This exchange is complete in $CaNd[CaRu]O_6$, as it was in $CaLa[CaRu]O_6$ (*1*), but only partial in $Ca_{1.46}Ho_{0.54}[Ca_{0.54}Ho_{0.46}Ru]O_6$, as it was in $CaNd[CaRu]O_6$, as it was in $CaLa[CaRu]O_6$ (*1*), but only partial in $Ca_{1.46}Ho_{0.54}[Ca_{0.54}Ho_{0.46}Ru]O_6$, as it was in $Ca_{1.43}Y_{0.57}[Ca_{0.57}Y_{0.43}Ru]O_6$ (*3*). Thus by choosing rare-earth ions of the appropriate size we have achieved our aim of controlling the distribution of magnetic ions within the unit cell. However, it appears that dilution of the magnetic species on the *B* site weakens the magnetic interaction between the rare-earth and Ru^{5+} to such an extent that the 6-coordinate rare earth ions in Ca_2HoRuO_6 remain paramagnetic, within the sensitivity limits of our experiment, at 4.2 K. This is perhaps surprising in view of the high magnetic moment of Ho^{3+} and the relatively large concentration of these ions remaining on the *B* sites. It is less surprising that the rare-earth ions on the *A* site in Ca_2NdRuO_6 also have an undetectable ordered magnetic moment at 4.2 K. The magnetic moments observed on the Ru^{5+} cations, which order in a Type I antiferromagnetic array in both Ca_2HoRuO_6 and Ca_2NdRuO_6, are again in good agreement with those reported previously.

In conclusion, we have described an example of magnetic coupling between a localized 4*f* electron system and a 4*d* electron system which is usually regarded as partially delocalized. We have shown that long range magnetic order can occur between the two cation types in a perovskite structure, but that this is dependent on the concentration and distribution of the rare-earth ions.

Acknowledgments

We are grateful to SERC for the provision of a research studentship to C.W.J. and to Dr. J. K. Cockcroft who gave experimental assistance at ILL, Grenoble.

References

1. P. D. BATTLE, J. B. GOODENOUGH, AND R. PRICE, *J. Solid State Chem.* **46,** 234 (1983).
2. P. D. BATTLE AND W. J. MACKLIN, *J. Solid State Chem.* **52,** 138 (1984).
3. P. D. BATTLE AND W. J. MACKLIN, *J. Solid State Chem.* **54,** 245 (1984).
4. P. D. BATTLE AND C. W. JONES, *J. Solid State Chem.* **78,** 108 (1989).
5. P. D. BATTLE, T. C. GIBB, C. W. JONES AND F. STUDER, *J. Solid State Chem.* **78,** 281 (1989).
6. B. C. TOFIELD, A. J. JACOBSON, AND B. E. F. FENDER, *J. Phys. C: Solid State Phys.* **5,** 2887 (1972).
7. W. C. KOEHLER, E. O. WOLLAN, AND M. K. WILKINSON, *Phys. Rev.* **118,** 58 (1960).
8. H. M. RIETVELD, *J. Appl. Crystallogr.* **2,** 65 (1969).
9. J. B. GOODENOUGH, "Magnetism and the Chemical Bond," Wiley, New York (1963).
10. M. K. WILKINSON, E. O. WOLLAN, H. R. CHILD, AND J. W. CABLE, *Phys. Rev.* **121,** 74 (1961).
11. M. BLUME, A. J. FREEMAN, AND R. E. WATSON, *J. Chem. Phys.* **37,** 1245 (1962).
12. C. W. JONES, Ph.D. Thesis, University of Leeds (1990).
13. Handbook on the Physics and Chemistry of the Rare Earths, (K. A. Gschneider and Le Roy Eyring, Eds.), Vol. III, North Holland (1979).